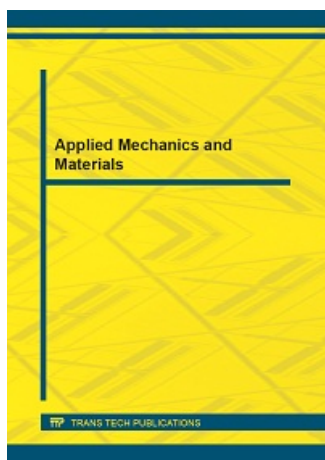


[./\(\)](#)中文 (<https://zh.scientific.net/AMM/Details>)
([/AN](#))[./Payment/Cart](#)LOG IN
(/ACCOUNT/LOG
RETURNURL=%2F

Search

Periodicals

Applied Mechanics and Materials

ISSN: 1662-7482[Volumes \(/AMM\)](#)[My eBooks \(/AMM/ebooks\)](#)[Details \(/AMM/Details\)](#)[Editorial Board \(/AMM/Editors\)](#)

About:

"Applied Mechanics and Materials" is a peer-reviewed journal which specializes in the publication of proceedings of international scientific conferences, workshops and symposia as well as special volumes on topics of contemporary interest in all areas which are related to:

- 1) Research and design of mechanical systems, machines and mechanisms;
- 2) Materials engineering and technologies for manufacturing and processing;
- 3) Systems of automation and control in the areas of industrial production;
- 4) Advanced branches of mechanical engineering such as mechatronics, computer engineering and robotics.

"Applied Mechanics and Materials" publishes only complete volumes on given topics, proceedings and complete special topic volumes. We do not publish stand-alone papers by individual authors.

Authors retain the right to publish an extended, significantly updated version in another periodical.

All published materials are archived with [PORTICO](http://www.portico.org/digital-preservation/who-participates-in-portico/participating-publishers/transtech) (<http://www.portico.org/digital-preservation/who-participates-in-portico/participating-publishers/transtech>) and [CLOCKSS](https://www.clockss.org/clockss/Participating_Publishers) (https://www.clockss.org/clockss/Participating_Publishers).

Authors can share research paper via KUDOS platform to help broaden your audience. Share your work via scholarly collaboration networks (like ResearchGate, Academia.edu and Mendeley) in a fully copyrightcompliant way using The Kudos Shareable PDF

Presented, Distributed and Abstracted/Indexed in:

SCImago Journal & Country Rank (SJR) www.scimagojr.com.

Inspec (IET, Institution of Engineering Technology) www.theiet.org.

Chemical Abstracts Service (CAS) www.cas.org.

Google Scholar scholar.google.com.

NASA Astrophysics Data System (ADS) <http://www.adsabs.harvard.edu/>.

Cambridge Scientific Abstracts (CSA) www.csa.com.

ProQuest www.proquest.com.

Ulrichsweb www.proquest.com/products-services/Ulrichsweb.html.

EBSCOhost Research Databases www.ebscohost.com/.

CiteSeerX citeseerx.ist.psu.edu.

Zetoc zetoc.jisc.ac.uk.

Index Copernicus Journals Master List www.indexcopernicus.com.

WorldCat (OCLC) www.worldcat.org.

ISSN print 1660-9336 ISSN cd 2297-8941 ISSN web 1662-7482

Additional Information:

Please ask for additional information: amm@scientific.net (<mailto:amm@scientific.net>)

Subscription

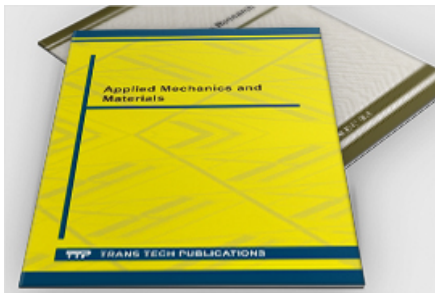
Irregular: approx. 20-30 volumes per year.

Rates 2019 for:

- Web 2019: EUR 1'154,-,

- Web 'All BackVolumes 2018-till Vol. 1': EUR 44'000,-,

- Print or CD 2019 (+free WEB): EUR 2'946,- (incl. Postage)



Share:

21

[DISTRIBUTION & ACCESS \(/DISTRIBUTOR\)](#)

[FOR PUBLICATION \(/FORPUBLICATION/CONFERENCE\)](#)

[SUPPLEMENTS \(/SUPPLEMENTS\)](#)

[ABOUT US \(/HOME/ABOUTUS\)](#)

[POLICY & ETHICS \(/POLICYANDETHICS/PUBLISHINGPOLICIES\)](#)

[CONTACT US \(/HOME/CONTACTS\)](#)

[IMPRINT & PRIVACY POLICY \(/HOME/IMPRINTANDPRIVACYPOLICY\)](#)

[SITEMAP \(/HOME/SITEMAP\)](#)

[_ \(https://www.facebook.com/Scientific.Net.Ltd/\)](https://www.facebook.com/Scientific.Net.Ltd/)

[_ \(https://twitter.com/Scientific_Net/\)](https://twitter.com/Scientific_Net/)

[\(https://www.linkedin.com/company/scientificnet/\)](https://www.linkedin.com/company/scientificnet/)

Scientific.Net is a registered brand of Trans Tech Publications Ltd
© 2019 by Trans Tech Publications Ltd. All Rights Reserved

Source details

Applied Mechanics and Materials

Scopus coverage years: from 2005 to 2015
(coverage discontinued in Scopus)

Publisher: Scitec Publications Ltd.

ISSN: 1660-9336

Subject area: Engineering: General Engineering

[View all documents >](#)

[Set document alert](#)

CiteScore 2015
0.07 ⓘ

SJR 2018
0.112 ⓘ

SNIP 2018
0.000 ⓘ

[CiteScore](#) [CiteScore rank & trend](#) [CiteScore presets](#) [Scopus content coverage](#)

CiteScore

2015

▼

Calculated using data from 31 May, 2016

0.07

=

Citation Count 2015

5,650 Citations >

Documents 2012 - 2014*

83,560 Documents >

*CiteScore includes all available document types

[View CiteScore methodology >](#)

[CiteScore FAQ >](#)

CiteScore rank ⓘ

Category	Rank	Percentile
Engineering		
General Engineering	#238/262	8th

[View CiteScore trends >](#)
[Add CiteScore to your site](#)

Metrics displaying this icon are compiled according to Snowball Metrics , a collaboration between industry and academia.

About Scopus

- What is Scopus
- Content coverage
- Scopus blog
- Scopus API
- Privacy matters

Language

- 日本語に切り替える
- 切换到简体中文
- 切换到繁體中文
- Русский язык

Customer Service

- Help
- Contact us

**SJR**

Scimago Journal & Country Rank

Enter Journal Title, ISSN or Publisher Name

[Home](#)[Journal Rankings](#)[Country Rankings](#)[Viz Tools](#)[Help](#)[About Us](#)

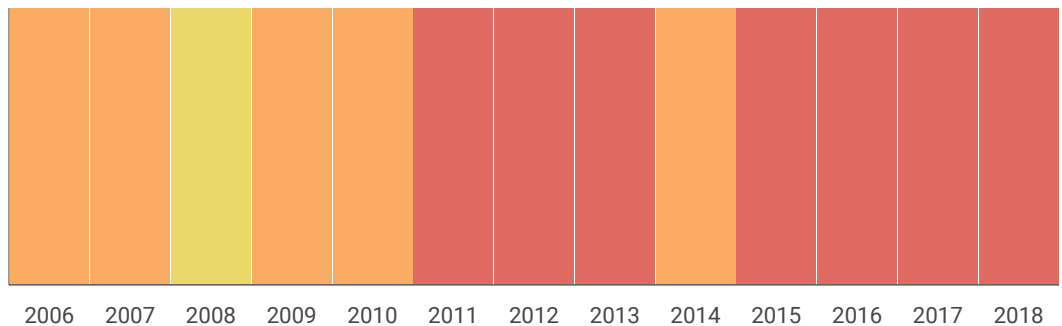
Applied Mechanics and Materials

Country [Switzerland](#) - [SJR Ranking of Switzerland](#)**Subject Area and Category** [Engineering](#)
[Engineering \(miscellaneous\)](#)**Publisher** [Scitec Publications Ltd.](#)**Publication type** Book Series**ISSN** 16609336**Coverage** 2005-2015 (cancelled)[Join the conversation about this journal](#)**28**

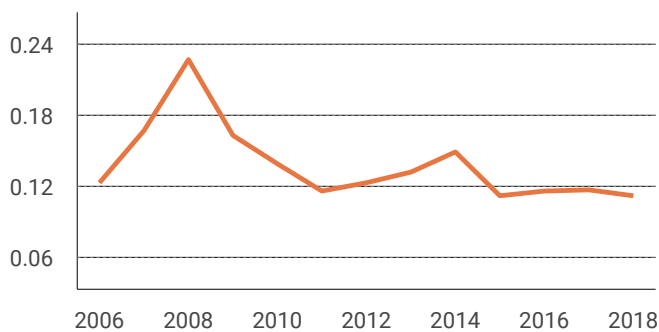
H Index

Quartiles

Engineering (miscellaneous)



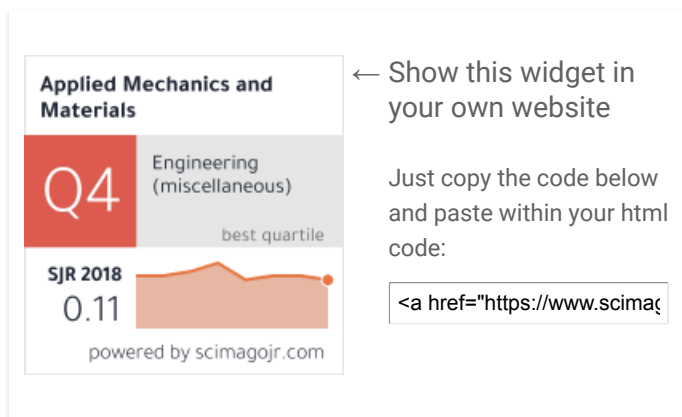
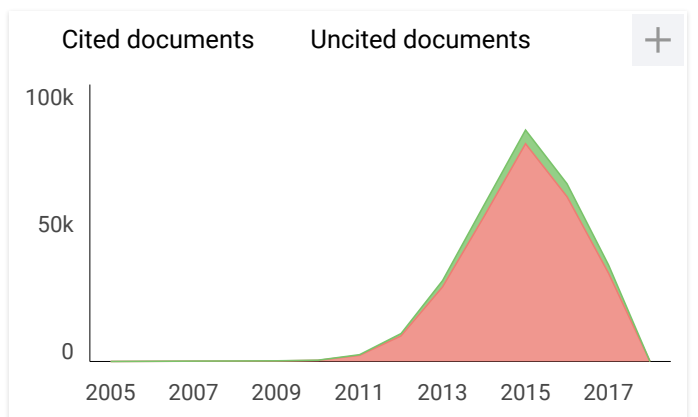
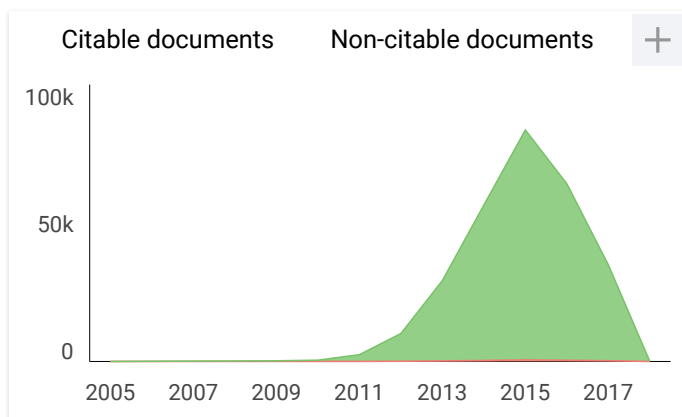
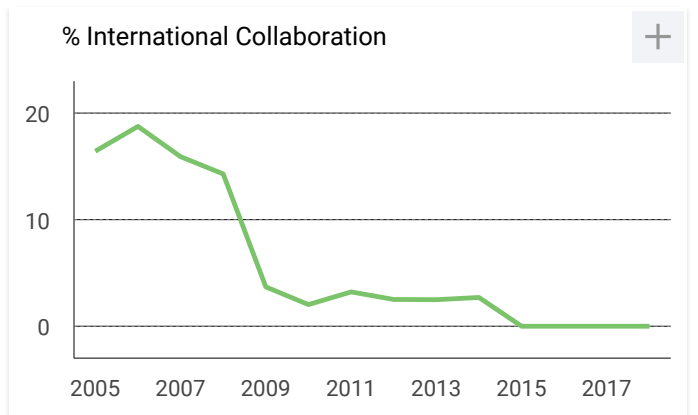
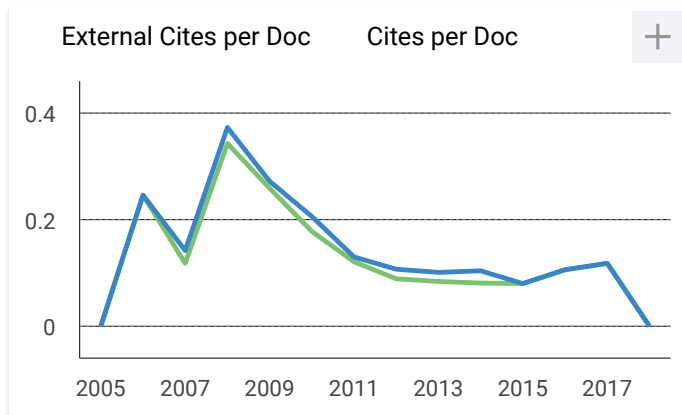
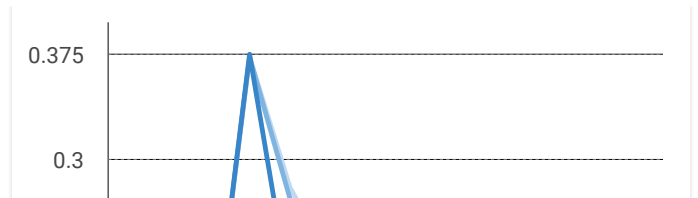
SJR



Citations per document

Total Cites

Self-Cites



O

ouarda rachidiou 2 months ago

i want to submit my paper in this journal

reply

D

Dr Medikundu Nageswara Rao 10 months ago

[./\(\)](#)[中文 \(https://zh.scientific.net/AMM/Editors\)](https://zh.scientific.net/AMM/Editors)
(/AN[./Payment/Cart\)](#)[LOG IN](#)
(/ACCOUNT/LOG
RETURNURL=%2F

Periodicals

Applied Mechanics and Materials

ISSN: 1662-7482

[Volumes \(/AMM\)](#)[My eBooks \(/AMM/ebooks\)](#)[Details \(/AMM/Details\)](#)[Editorial Board \(/AMM/Editors\)](#)

Editor(s) in Chief

Prof. Xi Peng Xu

Huaqiao University, Research Institute of Manufacturing Engineering at Huaqiao University; No.668, Jimei Road, Xiamen, China, 361021;

Editorial Board

Prof. Ezio Cadoni

University of Applied Sciences of Southern Switzerland, Department for Construction, Environment and Design, DynaMat Laboratory, SUPSI-DACD; Campus Trevano, Canobbio, 6952, Switzerland;

Dr. Yuan Sheng Cheng

Harbin Institute of Technology, School of Materials Science and Technology; P.O. Box 435, Harbin, China, 150001;

Dr. Dmitry A. Chinakhov

National Research Tomsk Polytechnic University, Yurga Institute of Technology (Branch); Leningradskaya 26, Yurga, Russian Federation, 652055;

Prof. Oana Dodun

Gheorghe Asachi Technical University of Iași, Department of Machine Manufacturing Technology; D. Mangeron Blvd, 39A, Iași, 700050, Romania;

Prof. Grigore Gogu

Institut Français de Mécanique Avancée, Campus de Clermont-Ferrand/les Cézeaux, CS 20265; Clermont-Ferrand, 63175, France;

Dr. Tibor Krenický

Technical University of Košice, Faculty of Manufacturing Technologies with a Seat in Prešov; Bayerova 1, Presov, 080 01, Slovakia;

Dr. Rozli Zulkifli

Universiti Kebangsaan Malaysia, Department of Mechanical and Materials Engineering, Faculty of Engineering and Built Environment;
Bangi, Malaysia, 43600;

[DISTRIBUTION & ACCESS \(/DISTRIBUTOR\)](#)

[FOR PUBLICATION \(/FORPUBLICATION/CONFERENCE\)](#)

[SUPPLEMENTS \(/SUPPLEMENTS\)](#)

[ABOUT US \(/HOME/ABOUTUS\)](#)

[POLICY & ETHICS \(/POLICYANDETHICS/PUBLISHINGPOLICIES\)](#)

[CONTACT US \(/HOME/CONTACTS\)](#)

[IMPRINT & PRIVACY POLICY \(/HOME/IMPRINTANDPRIVACYPOLICY\)](#)

[SITEMAP \(/HOME/SITEMAP\)](#)

[_ \(https://www.facebook.com/Scientific.Net.Ltd/\)](https://www.facebook.com/Scientific.Net.Ltd/)

[_ \(https://twitter.com/Scientific_Net/\)](https://twitter.com/Scientific_Net/)

[\(https://www.linkedin.com/company/scientificnet/\)](https://www.linkedin.com/company/scientificnet/)

Scientific.Net is a registered brand of Trans Tech Publications Ltd
© 2019 by Trans Tech Publications Ltd. All Rights Reserved

Table of Contents

Editorial Note

Chapter 1: Energy Conversion

Design of a Bubbling Fluidized Bed Gasifier for the Thermochemical Conversion of Oil Palm Empty Fruit Bunch Briquette A. Johari, B.B. Nyakuma, A. Ahmad, T.A.T. Abdullah, M.J. Kamaruddin, R. Mat and A. Ali	3
Laminar Flow Past a Circular Cylinder: Reduction of Drag and Fluctuating Lift Using Upstream and Downstream Rods D.Z. Noor, E. Widiyono, Suhariyanto, L. Rusdiyana and J. Sarsetiyanto	9
Trans-Esterification of Triglycerides with Methanol on Sulfated Zirconia Prepared with Different Concentration of Sulfuric Acid R. Mat, R.A. Samsudin, M. Mohamed, A. Johari, M.J. Kamaruddin and A. Ali	15
Numerical Studies on R22 Refrigerant Compressor Using Environment Friendly Working Fluids K.G.S. Shreenaath, J. Golecha, L.B. Augustin and M. Suresh	21
Case Studies Thermal Analysis of HP Condensate Stabilizer Column M. Qirom, A. Indarto and I.A. Putrawan	27
The Influence of Hydrogen Addition to Diesel Fuel Spray Combustion for Different Atomization Conditions N. Sriwardani, Y. Okamoto, T. Seo and M. Mikami	33
Hydrogen Production from Acetic Acid Steam Reforming over Bimetallic Ni-Co on La_2O_3 Catalyst-Effect of the Catalyst Dilution T.A.T. Abdullah, W. Nabgan, M.J. Kamaruddin, R. Mat, A. Johari and A. Ahmad	39
Driving Efficiency through Hydrocarbon for Green Car Air Conditioning A.A. Dahlan, H. Nasution, A.A. Aziz, Z.A. Latiff, M.R.M. Perang and A.Y. Wan Mohd	45
Air to Air Ejector with Various Divergent Mixing Chambers V. Dvořák	50
Kamojang Geothermal Power Plant Unit-1 : 30 Years of Operation R. Adiprana, D.S. Purnomo and I. Setiono	56
Flow Visualization Pattern on Sharp Edge T-Junction through Dividing Flow Channel Y.B. Lukiyanto, I.N.G. Wardana, W. Wijayanti and M.A. Choiron	62
An Experimental Study on the Vertical Flow Past a Finite-Length Horizontal Cylinder at Low Reynolds Numbers W. Stevanus and Y.J.P. Lin	68
Effect of Air Conditioning Position on Thermal Comfort in the Floor Air Conditioning System Y.A. Sabtalistia, S.N.N. Ekasiwi and B. Iskandriawan	74
Computational Fluid Dynamic Using Parallel Loop of Multi-Cores Processor C.L. Siow, Jaswar and E. Afrizal	80
Experimental Studies on a Solar Air Heater Having V-Corrugated Absorber Plate with Obstacles Bent Vertically E.A. Handoyo, D. Ichsan, Prabowo and Sutardi	86
Energy Savings in Air Conditioning System Using Ejector: An Overview K. Sumeru, L. Martin, F.N. Ani, H. Nasution and F.N. Ani	93
Empirical Correlations for Sizing Adiabatic Capillary Tube Using LPG as Refrigerant in Split-Type Air-Conditioner S. Sulaimon, A.A. Aziz, A.N. Darus and H. Nasution	99
Validation of AWTsim as Aerodynamic Analysis for Design Wind Turbine Blade I.K. Wiratama	105
Numerical Study on the Influence of the Corner Curvature of Circular Micropillar on Microdroplet Size via a Dewetting Process B.A. Dwiyantoro	111

Redesign ITS Central Library through Smart Building M. Junaidi, P. Kusriantoko, H. Ardhyanta, A. Bachtiar and A.A. Dimas	117
Optimization of Maximum Lift to Drag Ratio on Airfoil Design Based on Artificial Neural Network Utilizing Genetic Algorithm I. Haryanto, T.S. Utomo, N. Sinaga, C.A. Rosalia and A.P. Putra	123
Carbon Dioxide Effects on the Flammability Characteristics of Biogas N. Hamidi	129
Heat Transfer Effectiveness and Coefficient of Pressure Drop on the Shell Side of a Staggered Elliptical Tubes Bank U.K.W. Budi, K. Samsul, Suhanan and I.M. Suardjaja	134
Experimental Study on the Effect of Reynolds Number Variation on Drag Force for Various Cut Angle on D-Type Cylinders A. Pudjanarsa and A. Ardawalika	140
Performance of Conical Diffuser on Liquid Jet Gas Ejector D. Sugati, Indarto, Purnomo and Sutrisno	145
An Investigation into the Effect of Drag Coefficient on Overtaking of Car S.S. Al Homoud, D. Harmanto and I. Oraifge	151
Effects of Pine Oil on Dynamics of Bubble in Froth Flotation Warjito and I.P.A. Kautsar	155
Study on Auto-Ignition Behavior of Lubricating Oil in a Cone Calorimeter M.A.M. Siregar and Y.S. Nugroho	161
Solar Driven Absorption Chiller for Medium Temperature Food Refrigeration, a Study for Application in Indonesia I.N. Suamir	167
The Effect of Water Droplet Size on the Extinguished Concentric Jet Premixed and Diffusion Flame M.N. Sasongko	173
Gaining the Enthalpy of Solid Yields Formation in the Process of Waste Pyrolysis W. Wijayanti	179
Pipeline Leak Detection in Two Phase Flow Based on Fluctuation Pressure Difference and Artificial Neural Network (ANN) B. Santoso, Indarto and Deendarlianto	186
Reduction of Drag Force on a Circular Cylinder and Pressure Drop Using a Square Cylinder as Disturbance Body in a Narrow Channel W.A. Widodo and R.P. Putra	192
Experimental Study of Drag Reduction on Circular Cylinder and Reduction of Pressure Drop in Narrow Channels by Using a Cylinder Disturbance Body W.A. Widodo and N. Hidayat	198
Flammability Limit and Flame Visualization of Gaseous Fuel Combustion Inside Meso-scale Combustor with Different Thermal Conductivity L. Yuliati, M.N. Sasongko and S. Wahyudi	204
Energy Conversion in Compliance of Energy Self-Sufficient Village Program. Case Study: Jarak Village C. Meidiana, I.R.D. Ari and E.P. Paramita	210
Parallel Speed-Up of Preconditioned Fractional Step Navier-Stokes Solvers V. Djanali, S. Armfield, M. Kirkpatrick and S. Norris	215
Reactive Mixing Behavior of the Nitration of Glycerin in a Stirred Vessel at Various Perturbation R. Wulandari, I.N.G. Wardana, S. Wahyudi and N. Hamidi	221
Thermodynamic Analysis of Ejector as an Expansion Device on Split-Type Air Conditioner Using R410A as Working Fluid K. Sumeru, H. Nasution and F.N. Ani	227
Experimental Investigation on the Use of Secondary Refrigerant in Freezer for Energy Savings A.P. Haryono, E. Sukamto, Sumeru and F.N. Ani	233
Investigation of Natural Gas Composition Effects on Knock Phenomenon in SI Gas Engines Using Detailed Chemistry A. Javaheri, V. Esfahanian, A. Salavati-Zadeh, M. Darzi and S.M. Mirsoheil	239

Flow Characteristics around Four Circular Cylinders in Equispaced Arrangement near a Plane Wall	
A.G. Wailanduw, T. Yuwono and W.A. Widodo	245
Experimental Study on the Performance of In-Cabin Ventilation System	
Z. Abdul Latiff, C.W. Soon, B. Supriyo, M.R. Mohd Perang, H. Nasution and A.A. Aziz	251
Reduction of Energy Losses in the End Wall Junction Area through the Addition of Forward Facing Step Turbulent Generator	
H. Mirmanto, Sutrisno, H. Sasongko and D.Z. Noor	256
Biogas Potential of Co-Substrates in Balinese Biogas Plants	
D. Nett, I.N.S. Winaya, I.M.A. Putrawan, R. Wartmann and W. Edelmann	262
CFD Simulation of Heat Transfer in Fluidized Bed Reactor	
I.N.S. Winaya, I.M.A. Putrawan, I.N.G. Sujana and M. Sucipta	267
Influence of Bioethanol-Gasoline Blended Fuel on Performance and Emissions Characteristics from Port Injection Sinjai Engine 650 cc	
B. Sudarmanta, S. Darsopuspito and D. Sungkono	273
Improved Energy Saving for R22 Building Air Conditioning Retrofitted with Hydrocarbon Refrigerant, Study Case: Civil Engineering Department of ITS	
Widyastuti, A.B.K. Putra, R. Hantoro, E. Novianarenti and A.G. Safitra	281
The Evaluation of a Rigid Sail of Ship Using Wind Tunnel Test	
A. Sulisetyono	287
High-Efficiency Shrouded Micro Wind Turbine for Urban-Built Environment	
B. Kosasih and S.A. Jafari	294
Production of Ethanol as a Renewable Energy by Extractive Fermentation	
T. Widjaja, A. Altway, A.R. Permanasari and S. Gunawan	300
Kerosene-Water Flow Pattern in T-Junction Vertical Diameter Ratio 0.5 (Variation of Inclination Branch)	
D. Puspitasari, Indarto, Purnomo and Khasani	306

Chapter 2: Mechanical Design

Modeling and Analysis of Hybrid Shock Absorber for Military Vehicle Suspension	
H.L. Guntur, W. Hendrowati and T. Budiarto	315
Design Online Artificial Gain Updating Sliding Mode Algorithm: Applied to Internal Combustion Engine	
A. Priyanto, M.J. Nekooei and Jaswar	321
Optimization Spring Coil Design for Orthodontic Tooth Movement	
M.A. Choiron, E. Sutikno, T.H. Wicaksono and S. Haruyama	327
Thermal Stress Intensity Factors of Crack in Solid Oxide Fuel Cells	
K. Anam and C.K. Lin	331
Intelligent Bearing Diagnostics Using Wavelet Support Vector Machine	
A. Widodo, I. Haryanto and T. Prahasto	337
Degradation Trend Estimation and Prognosis of Large Low Speed Slewing Bearing Lifetime	
B. Kosasih, W. Caesarendra, K. Tieu, A. Widodo, C.A.S. Moodie and A.K. Tieu	343
Electrical Energy from Vibration of a Washing Machine	
B.D. Wonoyudo and T. Febrawi	349
Computer Assisted Fracture Reduction and Fixation Simulation for Pelvic Fractures	
P.Y. Lee, J.Y. Lai, C.Y. Huang and Y.S. Hu	354
Structural Analysis of a Tracking Photovoltaic System with a Pedestal Solar Tracker	
C.K. Lin and C.Y. Dai	361
New Polyhedral Elements Based on Virtual Node Method for Solid Mechanics and Heat Transfer Applications	
L. Perumal and M.I. Fadhel	367
Experimental Study of Vibration of Prototype Auditory Membrane	
H. Tanujaya and S. Kawano	372
Interaction between a Crack and an Isotropic Tri-Material Media in Anti-Plane Elasticity	
A. Wikarta and C.K. Chao	378

Split Bar Hopkinson with Springs Striker Bar Launcher A.S. Pramono, Sujarwanto and H. Rivazani	383
Neural Network-Based Engine Propeller Matching (NN-EPM) for Trimaran Patrol Ship E.S. Koenhardono, E.B. Djatmiko, A. Soeprijanto and M.I. Irawan	388
Modeling, Prototyping and Testing of Regenerative Electromagnetic Shock Absorber A.I. Sultoni, I.N. Sutantra and A.S. Pramono	395
Designing and Prototyping Surveillance Robot with Self-Protection Using Nail Gun N. Sebastian, Erwin, E. Listijorini and Dwinanto	401
Numerical Modelling of the Initial Stress and Upward Deflection of Glulam Beams Pre-Stressed by Compressed Wood B. Anshari and Z.W. Guan	408
Modular System for Testing the Performance of Poly-Articulate Robotic Structures V.C. Dumitru	414
Preliminary Numerical Study on Designing Navigation and Stability Control Systems for ITS AUV T. Herlambang, H. Nurhadi and Subchan	420
Numerical Study of Salat Movements for Total Hip Replacement Patient R. Ismail, E. Saputra, M. Tauviquirrahman, A.B. Legowo, I.B. Anwar and J. Jamari	426
Physiological Concept: Visible Modeling for Feasible Design C.P.M. Sianipar, G. Yudoko and K. Dowaki	432
Actuator Power Consumption of Active Suspension System with Override Control Strategy U. Wasiwitono	438
Trailing Edge Deformation Mechanism for Active Variable - Camber Wind Turbine Blade B. Kosasih and M. Dicker	444

Chapter 3: Manufacturing Processes and Technologies

Effect of Material and Process Parameter on Dimensions of Rolled External Threads P.S. Chauhan, C.M. Agrawal and R.K. Dwivedi	453
The Emergy Value Assessment of Municipal Waste Management in Yogyakarta, Indonesia C. Meidiana	461
Evaluation of the Effect of Application of Air Jet Cooling and Cooled-Air Jet Cooling on Machining Characteristics of St 60 Steel Rusnaldy, N. Iskandar, Y. Umardani, Paryanto and S.A. Widyanto	468
Simulation of Semi-Active the Blank Holder Force Control to Prevent Wrinkling and Cracking in Deep Drawing Process S. Candra, I.M.L. Batan, W. Berata and A.S. Pramono	473
System Architecture and FPGA Embedding of Compact Fuzzy Logic Controller for Arm Robot Joints B. Siswoyo, M.A. Choiron, Y.S. Irawan and I.N.G. Wardana	480
Organizational Culture in Manufacturing Company: Study Case of Small and Medium Sized Enterprises in Central Java, Indonesia H. Lestari, R. Ismail and A. Mansur	486
Development Machining of Titanium Alloys: A Review M. Darsin and H.A. Basuki	492
Modal and Harmonic Response Analysis: Linear-Approach Simulation to Predict the Influence of Granular Stiffeners on Dynamic Stiffness of Box-Shaped Workpiece for Increasing Stability Limit against Chatter O. Soegihardjo, Suhardjono, B. Pramujati and A.S. Pramono	501
The Preliminary Research of Drill Guide Template Design for Pedicle Screw Placement with a Low-Cost 3D Pinter C.Y. Liao, C.J. Cheng, W.J. Huang and C.M. Cheng	507
Experimental-Based TGPID Motion Control for 2D CNC Machine H. Nurhadi, Subowo, S. Hadi and M. Mursid	511
Preliminary Study on Magnetic Levitation Modeling Using PID Control D.A. Patriawan, B. Pramujati and H. Nurhadi	517

Multiple Performance Optimization in the Wire EDM Process of SKD61 Tool Steel Using Taguchi Grey Relational Analysis and Fuzzy Logic N. Lusi, B.O.P. Soepangkat, B. Pramujati and H.C.K. Agustin	523
Optimization of Recast Layer Thickness and Surface Roughness in the Wire EDM Process of AISI H13 Tool Steel Using Taguchi and Fuzzy Logic P. Rupajati, B.O.P. Soepangkat, B. Pramujati and H.C.K. Agustin	529
Optimization of Tool Wear, Surface Roughness and Material Removal Rate in the Milling Process of Al 6061 Using Taguchi and Weighted Principal Component Analysis (WPCA) L. Ulfiyah, B. Pramujati and B.O.P. Soepangkat	535
Design and Application of the Stretching Technology on the Welding Process of Stiffened Sheet Metal Structure H. Sukanto, Triyono and N. Muhayat	541
Effect of High Speed Dry End Milling on Surface Roughness and Cutting Forces of Ti-6Al-4V ELI S. Sharif, H. Safari, S. Izman and D. Kurniawan	546
Visible Light Maskless Photolithography for Biomachining Application D. Suwandi, Y. Whulanza and J. Istiyanto	552
Improvement of Tungsten Inert Gas (TIG) Welding Penetration Using the Effect of Electromagnetic Field A.S. Baskoro, Tuparjono, Erwanto, S. Frisman, A. Yogi and Winarto	558
Response of Grip Force as Effect of Electrics Power Input at Gripper Actuator of NiTi SM495 Wire T. Oerbandono and H. Budiarto	564
Image Processing Implementation in Measurement of Cross-Flow Water Turbine Geometry A. Wahjudi, I.M.L. Batan, B.M. Pradnyana and W. Rusweki	570
Application of Semi Automatic Model of Product Complexity Index Calculation by Identification and Recognition of Geometric Features Information H.D.S. Budiono, M. Sholeh, G. Kiswanto and T.P. Soemardi	576
Multiple Performance Characteristics Optimization in the Turning Process of AISI H13 Tool Steel Using Taguchi and Fuzzy Logic B.O.P. Soepangkat, B. Pramujati and B.W. Karuniawan	583
Numerical Simulation of Multipoint Forming with Circular Die Pins in Hexagonal Packing W. Rivai, S. Putu, B.L. Sanjoto, H. Nur and S. Hari	589
Design of Multi Gender Bicycle - As an Alternative Bike Design to Fulfill Appropriate Requirement for Urban Society in Indonesia I.M.L. Batan and R. Hendarto	594

Chapter 4: Material Science and Engineering

Sol-Gel Synthesis of Zn Doped HA Powders and their Conversion to Porous Bodies A. Naqshbandi, I. Sopyan, Gunawan and Suryanto	603
Synthesis and Characterization of Zinc Oxide Nanoparticles via Self-Combustion Technique P. Puspitasari, Andoko and E. Sutadji	609
Effect of Ingredients on Flexural Strength of Friction Composite Jamasri, V. Malau, M.N. Ilman and E. Surojo	615
Dielectric Properties for the Ring Opening Polymerisation of ϵ-Caprolactone M.J. Kamaruddin, M.A.A. Zaini, A. Johari and T.A.T. Abdullah	621
P-h Curves and Hardness Value Prediction for Spherical Indentation Based on the Representative Stress Approach I.N. Budiarsa and M. Jamal	628
Simple Recipe to Synthesize BaTiO₃-BaFe₁₂O₁₉ Nanocomposite Bulk System with High Magnetization D. Suastiyantia, B. Soegijono and M. Hikam	634
Effect of Cellulose Acetate Phthalate (CAP) on Characteristics and Morphology of Polysulfone/Cellulose Acetate Phthalate (PSf/CAP) Blend Membranes A. Ali, R.M. Yunus, M. Awang, A. Johari and R. Mat	640

Analysis of Fiber Glass/Vinyl Ester Composite Subjected to Internal Pressure Loading for Compressed Natural Gas (CNG) Tube Type IV Application H. Ardhyanta, R.N. Baiti, M. Adi Afrianto and D. Kurniawan	645
Microstructure Study on Fe/Cr Based Alloys Added with Yttrium Oxide (Y_2O_3) Prepared via Ultrasonic Technique for Solid Oxide Fuel Cell (SOFC) Application D. Feriyanto, M.I. Idris, D. Sebayang, A. Bin Otman and P. Untoro	651
Microstructure and Magnetic Properties of Barium Hexaferrite Produced by Sol Gel Auto Combustion for Radar Absorber Material (RAM) Application Widyastuti, E. Kharismawati, M. Zainuri and H. Ardhyanta	656
The Influence of Carboxy Methyl Cellulose (CMC) and Solution pH on Carbon Fiber Dispersion in White Cement Matrix A.Y. Akbar, Y. Lestari, G. Ramadhan, S.A. Candra and E. Sugiarti	661
Effects of Heat Treatment and Titanium Nitride (TiN) Coating Deposited by Sputtering Technique PVD on Duylos 2510 Tool Steel Substrate V. Malau, S. Subagyo and Supriyanto	666
Experimental Study of Impact on Carbon-Fiber-Epoxy Composite Wing Leading Edge Structure N. Omar, Y. Aminanda and J.S. Mohamed Ali	672
Acoustic Emission Hit Generation Behavior of Basalt Fiber High Strength Mortar under Compression N.N. Kencanawati and M. Shigeishi	678
Application of Myrmecodia Pendans Extract as a Green Corrosion Inhibitor for Mild Steel in 3.5% NaCl Solution A. Pradityana, S. Sulistijono and A. Shahab	684
$Al_2O_3 - SiO_2$ Coating by Flame Spray for Thermal Barrier Coating Application Widyastuti, L. Mariani, S. Ridwan and M.A. Putrawan	691
Sintering of Stainless Steel Nanopowders for Micro-Component Part Applications S. Supriadi and E.R. Baek	697
Effect of Electron Beam Irradiation on Mechanical and Thermal Properties of Ethylene Vinyl Acetate/Polyamide 6/High Density Polyethylene Nanocomposite F. Hamid, S. Akhbar, K.H. Ku Halim and A.R.M. Faizal	703
Effect of Tool Tilt Angle and Tool Plunge Depth on Mechanical Properties of Friction Stir Welded AA 5083 Joints N. Muhayat, A. Zubaydi, Sulistijono and M.Z. Yuliadi	709
Preliminary Study of Development of HDPE/EVA/MMT/EFB Nanohybrid Biocomposite by Using Single Screw Extruder M.S. Jainal, S.N. Che Kamarludin, S. Akhbar and A.R.M. Faizal	715
Effect of Intercritical Annealing Temperature and Holding Time on Microstructure and Mechanical Properties of Dual Phase Low Carbon Steel Alfirano, W. Samdan and H. Maulud	721
The Influence of High Content of Silicon in Austenitic Stainless Steel to Corrosion Rate in Sulphuric Acid F. Gapsari, S. Wahyudi and Sumawan	727
Optimization of Chemical Environment Condition towards Corrosion Rate of Sulfuric Acid Resistant Alloy Metal (Saramet) Using Response Surface Methodology S. Wahyudi, F. Gapsari and H. Awali	733
Effects of High Speed Tool Rotation in Micro Friction Stir Spot Welding of Aluminum A1100 A.S. Baskoro, Suwarsono, G. Kiswanto and Winarto	739
Slump Flow Modeling of Self-Compacting Concrete Using Smooth Support Vector Regression (SSVR) Y.S. Hadiwidodo and S.W. Purnami	743
Hydrophobic Silica Coating Based on Waterglass on Copper by Electrophoretic Deposition E. Setyowatia, S.F. Amalia, Nazriati, S. Affandi, M. Yuwanae and H. Setyawan	749
Comparison of AISI 316L Plasma Nitriding Behavior in Low and Medium Temperature Istiroyah, I.N.G. Wardana and D.J. Santjojo	755
Na_2SO_4 Induced Hot Corrosion of Aluminized Low Carbon Steel at 700 °C M. Badaruddin	761

Development and Evaluation of Nano Electret Filters for Household Water Treatment

Y.C. Ahn, J.I. Cho, S.E. Kim, A.H. Jeong and G.T. Kim

767

Effect of Starter Defect to G_{IIC} of Unidirectional CFRP Composite

F.M. Nor, H.Y. Lee, J.Y. Lim, M.N. Tamin and D. Kurniawan

773

Effect of Heat Treatment on Microstructure Homogeneity of Zn-3Mg Alloy

M.S. Dambatta, S. Izman, H. Hermawan and D. Kurniawan

777

Experimental Studies on a Solar Air Heater Having V-Corrugated Absorber Plate with Obstacles Bent Vertically

Ekadewi A. Handoyo^{1,2,a}, Djatmiko Ichsani^{1,b}, Prabowo^{1,c}, Sutardi^{1,d}

¹Mechanical Engineering Dept, Institut Teknologi Sepuluh Nopember, Surabaya – Indonesia

²Mechanical Engineering Dept, Petra Christian University, Surabaya – Indonesia

^aekadewi@peter.petra.ac.id, ^bdjtmiko@me.its.ac.id, ^cprabowo@me.its.ac.id, ^dsutardi@me.its.ac.id

Keywords: solar air heater, obstacle, solar collector, v-corrugated absorber plate.

Abstract.

A solar air heater (SAH) is a simple heater using solar radiation that is useful for drying or space heating. Unfortunately, heat transfer from the absorber plate to the air inside the solar air heater is low. Some researchers reported that obstacles are able to improve the heat transfer in a flat plate solar air collector and others found that a v-corrugated absorber plate gives better heat transfer than a flat plate. Yet, no work of combining these two findings is found.

This paper describes the result of experimental study on a SAH with v-corrugated absorber plate and obstacles bent vertically started from 80° to 0° with interval 10° on its bottom plate. Experiments were conducted indoor at five different Reynolds numbers ($1447 \leq Re \leq 7237$) and three different radiation intensities (430, 573, and 716 W/m²).

It is found that the obstacles improve SAH performance. Both the air temperature rise and efficiency increase with inserting obstacles bent at any angle vertically. Unfortunately, the air pressure drop is increasing, too. Obstacles bent vertically at smaller angle (means more straight) give higher air temperature rise and efficiency. However, the optimum angle is found 30°. The air temperature rise and efficiency will be 5.3% lower when the obstacles bent 30° instead of 0°, but the pressure drop will be 17.2% lower.

Introduction

As a country located in Equator, there is a lot of sunshine on surfaces in Indonesia. The sun's radiation energy can be converted into thermal energy by means of a solar collector. The sunlight transmitted by cover glass falls onto a plate which absorbs the heat. This absorber plate transfers the heat to the working fluid which is either water or air. Water has better thermal storage and higher convective heat transfer coefficient than air. Yet, air is much lighter and less corrosive than water. Furthermore, the heated air can directly be used for drying some farming product such as grain. Generally, the solar air heater is less efficient than the solar water heater, because air has less thermal capacity and less convection heat transfer coefficient. These encourage some research in solar air heater (SAH).

Most of SAH being investigated is flat plate type. It has a cover glass on the top, insulation on the sides and bottom to prevent heat transferred to the surrounding, a duct for the air flowing and an absorber flat plate. The air can flow over and/or under the absorber plate. To increase the convection heat transfer from the absorber plate to the air, a v-corrugated plate is used instead of a flat plate. SAH with a v-corrugated absorber plate can reach efficiency 18% higher than the flat plate under the same operation and condition [1]. A solar collector with a v-corrugated absorber is 10–15% and 5–11% more efficient in single pass and double pass modes, respectively, compared to the flat plate collectors [2]. For the same length of collector, mass flow rate, and air speed, it was found out that the corrugated and double cover glass collector gave the highest efficiency [3]. The results of mathematical simulation and experiment show that v-corrugated absorber was found to be more efficient than flat plate collector [4]. The corrugated surfaces give a significant effect on the enhancement of heat transfer and pressure drop. The Nusselt number of flow in a v-corrugated channel can increase to 3.2 – 5.0 times higher than in a plane surfaces while the pressure drop 1.96 times higher than on the corresponding plane surface [5]. The corrugated channel gave higher Nusselt

number than the straight channel and a higher channel height gave higher Nusselt number for the flow with the same Reynolds number [6].

Besides increasing the heat transfer surface area, some also give effort to increase turbulence inside the channel with fins or obstacles. The result of experimental study done in turbulent flow regime (Reynolds number of 5000 to 25,000) showed that multiple 60° V-baffle turbulator fitted on a channel provides the drastic increase in Nusselt number, friction factor, and the thermal enhancement factor values over the smooth wall channel [7]. From the research of two kinds of rectangular fins which dimension are different but total area are the same, it was found that collector with fins type II, both free and fixed, was more effective than type I and flat-plate collector. The fixed fin collector was more effective than free fin collector [8]. The efficiency of collector and the air temperature was found increasing with the use of baffles. Baffles should be used to guide the flow toward the absorber plate [9]. The experiment and theoretical investigations gave result that heat transfer was improved by employing baffled double-pass with external recycling and fins attached over and under absorber plate [10]. The obstacles on the flat plate reduced the grape drying time, because they ensure a good air flow over the absorber plate, create the turbulence and reduce the dead zones in the collector [11]. From research on three-passages SAH with three different type obstacles placed on absorber plates, it was found that type III obstacles with flow in middle passage gave the highest efficiency and all collectors with obstacles gave higher efficiency than the flat plate [12]. The optimal value of efficiency was obtained for SAH with Type II obstacles on absorber plate in flow channel for all operating conditions and the collector with obstacles appears significantly better than that without obstacles [13]. The delta-shape obstacle mounted on the absorber surface enhances the heat transfer to the air and the heat transfer was higher if the obstacle was taller and its longitudinal pitch was smaller [14].

There are two findings that are important. First, the obstacles are able to enhance heat transfer in a flat plate collector and second, a v-corrugated plate gives better heat transfer than a plane duct. It is necessary to study the combination of these two findings. Since pressure drop is an important parameter in SAH, it is interesting to study the effect of bending the obstacles vertically, too. This paper describes the result of experimental study on a SAH with v-corrugated absorber plate and obstacles bent vertically on its bottom plate.

Experimental set-up

A small scale model of a SAH having v-corrugated absorber plate has been set up indoor. Its schematic view and photograph are shown in Fig. 1. The experiments were conducted in a laboratory of Mechanical Engineering Dept of Petra Christian University, Surabaya, Indonesia.

The solar collector's model was constructed with its bottom plate can be replaced with other plate having obstacles on it. The dimension of the model was 900 mm x 90 mm x 125 mm. The cover of the collector was made of a single 3-mm transparent-tempered glass. Black painted aluminum was used as the v-corrugated absorber plate. The apex angle of the v-corrugated plate was 20°. The dimension of the absorber plate was 900 mm long, 87 mm hypotenuse, and 0.8 mm thick. The v-corrugated duct's cross section dimension was 30 mm width and 85 mm height. To prevent heat loss, the left and right walls of collector are insulated with a 25-mm Styrofoam each and a 35-mm Styrofoam for the bottom. The obstacles used were isosceles triangular plate with dimension are 18 mm wide and 51 mm height. The ratio of spacing to height of obstacles in sequence, S/H, equal to 1 or the percentage of air flow blockage in the channel was 36% when the obstacles are straight. Thus, there are 17 obstacles. In the experiment, the obstacles were bent vertically with angle started from 80° to 0° with interval 10°. Obstacles with angle 0° mean they are straight, not bent. Thus, there are nine set of obstacles inserted on the bottom plate as shown in Fig. 1 (d).

The experiments were set up indoor to ensure the same radiation intensity, wind's speed and ambient temperature. So, a bias result that effected by different outdoor condition can be avoided. The artificial sunlight was modeled by four 500-Watt halogen lamps. A pyranometer (Kipp & Zonen, type SP Lite2) placed on top of the cover glass was used to measure the radiation intensity received on the collector. To ensure the homogenous intensity and to generate some different intensity received

on the collector, these lamps were equipped with adjustable turner individually. The experiments were conducted on three different radiation intensities, i.e. 430, 573, and 716 W/m².

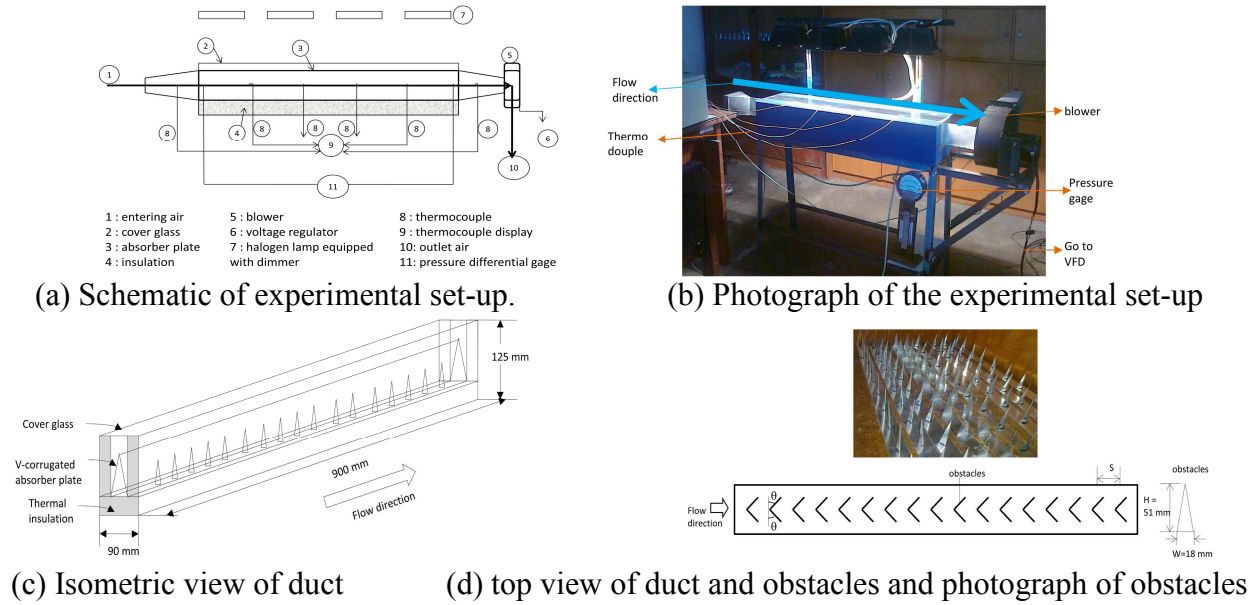


Fig. 1. Experimental set-up.

The temperature, humidity, and wind speed of air surrounding were well controlled. Some T-type thermocouple which accuracy are 0.1°C are used to measure temperature of flowing air at inlet and outlet of the collector, temperature of the absorber plate (at four different locations). Each thermocouple has its own display. The pressure drop between inlet and outlet of the flowing air across the collector was also measured with a Magnehelic differential pressure gage which accuracy is 2 Pa and manometer using oil which accuracy is 1 mm. A centrifugal blower was used to induce the air flowing in the channel (1000 m³/h, 580 Pa, 0.2 kW, 380 Volt input). The air flow speed was controlled by adjusting the motor's frequency using a variable-frequency drive (VFD). The experiments were performed at five different air inlet velocities, i.e. 1.0 m/s, 2.0 m/s, 3.0 m/s, 4.0 m/s, and 5.0 m/s or at Reynolds number of 1447, 2895, 4342, 5790, and 7237, respectively. The air speed was measured using digital anemometer which accuracy is 0.1 m/s.

The experiment was conducted on model without any obstacle and consecutively with obstacles bent with some angles. Thus, there are ten set experiments conducted for each air flow speed and radiation intensity. A VFD was used to adjust the frequency of the blower's motor to ensure a constant air flow speed during the experiment.

When the inlet and outlet temperature (T_i , T_o , respectively) and the mass flow rate of air (\dot{m}_f) are known from experiments and the value of air specific heat (c_p) is known, then the useful energy rate (\dot{Q}_u) can be calculated using Eq. (1).

$$\dot{Q}_u = \dot{m}_f c_p (T_o - T_i). \quad (1)$$

According to [15], this useful energy can be expressed in terms of energy absorbed by the plate from radiation received (I) and energy lost from the absorber, as given by Eq. (2).

$$\dot{Q}_u = F_R \tau \alpha A_c I - F_R U_L A_c (T_i - T_a). \quad (2)$$

The instantaneous efficiency of a collector relates the useful energy to the total radiation received on the collector surface as shown in Eqs. (3) and (4) [15].

$$\eta = \frac{\dot{Q}_u}{I A_c} = \frac{\dot{m}_f c_p (T_o - T_i)}{I A_c} \quad (3)$$

$$\eta = \frac{\dot{Q}_u}{I A_c} = F_R (\tau \alpha) - F_R U_L \frac{(T_i - T_a)}{I}. \quad (4)$$

In Eq. (4), the useful energy depends on parameters of construction material of the SAH and flow conditions, i.e. F_R , the collector heat removal factor, U_L , total heat loss coefficient, A_c , collector area, and $(\tau \alpha)$, transmittivity of the glass cover times absorptivity of the absorber plate.

The inlet air temperature, T_i , usually equals to the ambient temperature, T_a , during experiments. Thus, Eq. (4) is modified to be Eq. (5) [15].

$$\eta = \frac{\dot{Q}_u}{I A_c} = F_o \tau \alpha - F_o U_L \frac{(T_o - T_a)}{I} \quad (5)$$

Eq. (5) specifies that a plot of instantaneous efficiency as a function of $\frac{(T_o - T_a)}{I}$ will result a straight line which slope and intercept are $F_o U_L$ and $F_o \tau \alpha$. F_o is the collector heat gain factor. If the optical properties of the SAH, ($\tau \alpha$), are known, then F_o and U_L can be determined.

Results and discussion

The experiments were conducted on three different radiation intensities and five different air flow speed. The performance of SAH includes the air temperature rise, instantaneous efficiency, and air pressure drop. The air temperature rise is determined from $(T_o - T_i)$ and the instantaneous efficiency is calculated using Eq. (5). The pressure drop is measured directly during experiments.

The radiation received on the absorber plate and the air flow rate crossing the SAH affect the rise of air temperature as shown in Fig. 2. It is higher when the air flow is lower at any radiation intensity and when the radiation intensity is larger at any air flow speed. Without any obstacle, SAH gave the lowest air temperature rise of 12.7°C and the highest of 25.2°C. The lowest air temperature rise is obtained at the lowest radiation intensity (430 W/m²) and the largest air flow speed (5.0 m/s). The highest rise is acquired at the largest radiation intensity (716 W/m²) and the smallest air flow speed (1.0 m/s). Obstacles increase the air temperature rise whether they are bent or straight. The straight (0° obstacles) increase the lowest air rise from 12.7°C to 16.2°C and the highest air rise from 25.2°C to 34.9°C.

The air temperature rise in Fig. 2 and SAH's instantaneous efficiency in Fig. 3 decrease as the obstacles bent at larger angle. Fig. 2 show that the air temperature rise is almost the same when the obstacles bent at 30°, 20°, 10°, or 0° (straight) but the pressure drop is quite different as shown in Fig. 4. The air temperature rise and efficiency will be 5.3% lower when the obstacles bent 30° instead of 0°, but the pressure drop will be 17.2% lower.

Obstacles inserted in the flow generate turbulence and focus the air flow toward the absorber plate. When the obstacles slightly bent vertically, the air flow becomes obstructed. Some of the air will flow back causing the flow to recirculate and will reattach downstream before the next obstacles. This creates vortex near the obstacles and increase the turbulence in the air flow. Some of the air will flow in the small gap between the obstacles and absorber plate. This small gap forces the air to stay in contact with the absorber plate and to increase its velocity and turbulence. These make the heat transfer to the air flow and air pressure drop through collector increase when there are obstacles slightly bent vertically. There is something unpredictable happened, i.e. when the air flow is small (1.0 and 2.0 m/s), the temperature rise is very low as the obstacles bent at angle 10° at any radiation intensity. This phenomenon needs further research and numerical study or visualization to learn the flow around the 10° obstacles.

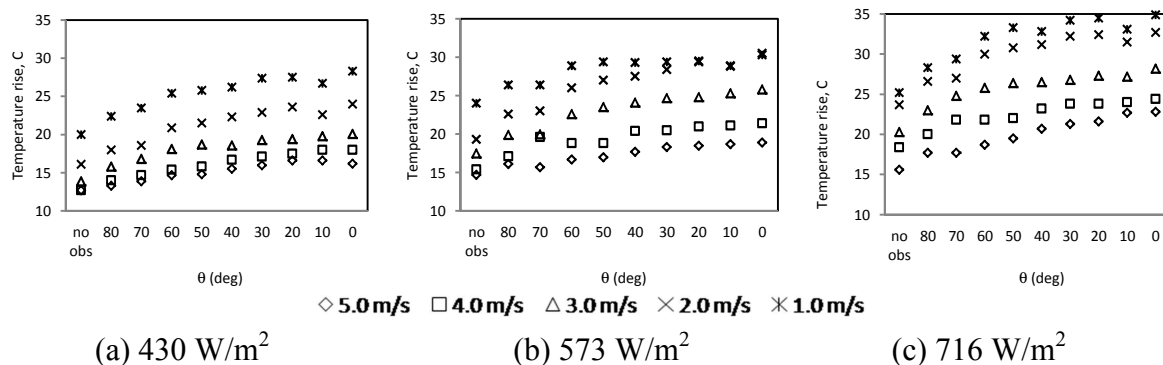


Fig. 2. The rise of air temperature at some air flow and radiation intensity for many configurations.

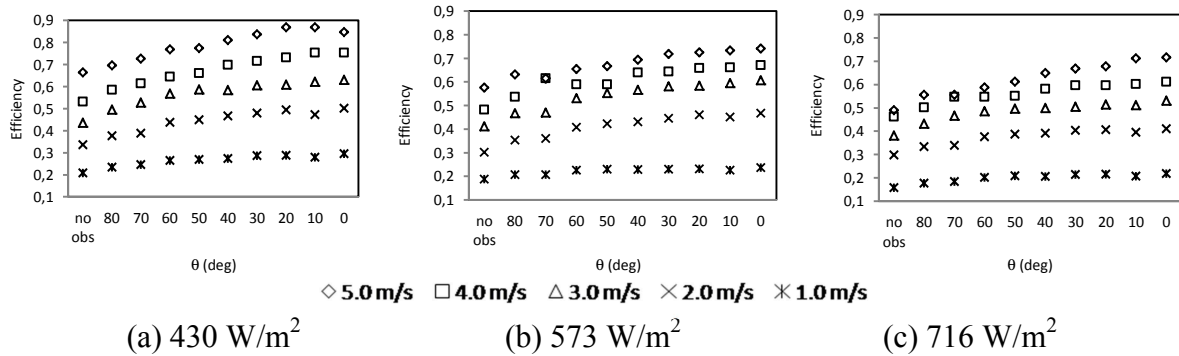


Fig. 3. Efficiency of SAH at some air flow and radiation intensity for many configurations.

The efficiency of the collector calculated using Eq. (3) shown in Fig. 3 give the consistent result with Fig. 2. As air temperature rise increased, the efficiency of the collector having obstacles also improved. For example, when inlet air speed is 5.0 m/s and radiation is 573 W/m², the efficiency of solar air heater with straight obstacles can reach 0.742 (74.2%) while it was only 0.577 (57.7%) when no obstacle used. The efficiency has the same trend with temperature rise, i.e. it is almost the same when the obstacles bent at 30°, 20°, 10°, or 0° (straight).

The static pressure of the air drops as it flows through the channel made by the v-corrugated absorber plate and the bottom plate. Fig. 4 shows the pressure drop for the ten SAH. To see the pressure drop more clearly, the graphs are separated, one for air flow speed of 1.0 and 2.0 m/s as in Fig. 4 (a), and one for air flow speed of 3.0 m/s, 4.0 m/s, and 5.0 m/s as in Fig. 4 (b). The pressure drop can decrease 17.2% when the obstacles bent at 30 degree instead of 0 degree when the air flow speed 5.0 m/s.

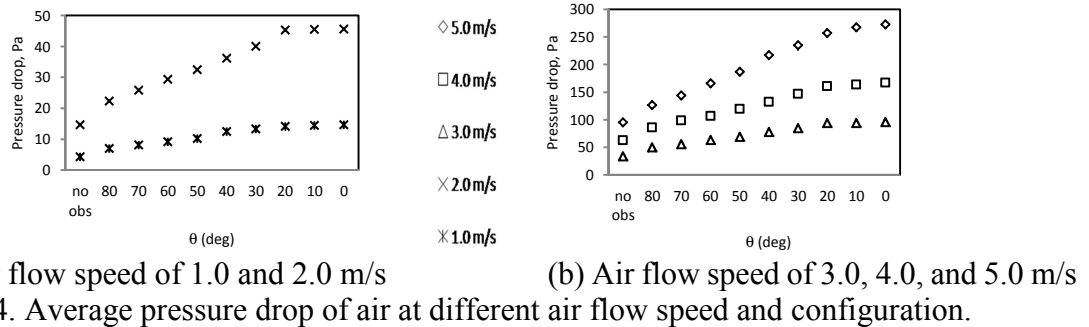


Fig. 4. Average pressure drop of air at different air flow speed and configuration.

The efficiency of SAH can be calculated using Eq. (5) as shown if Fig. 5. Due to space limitation, only two configurations of ten (no obstacle and 0° obstacles) are shown. When some 0° obstacles are inserted on the bottom plate, the efficiency is much higher than without obstacles. The slope of the linear regression is $F_o U_L$ and the intercept with vertical axis is $F_o \tau \alpha$.

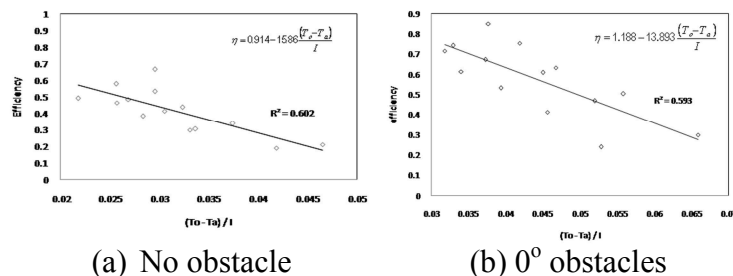


Fig. 5. Efficiency of SAH with the temperature parameter $(T_o - T_a)/I$ at two configurations.

Using data that transmissivity (τ) of tempered glass is 0.87 and absorptivity (α) of aluminum plate is 0.92, then the collector heat gain factor (F_o) and the total heat loss coefficient (U_L) can be calculated as shown in Fig. 6. SAH without obstacle has the lowest F_o and the maximum U_L . The heat gain factor (F_o) increases and total heat loss coefficient (U_L) decreases as the obstacles bent at smaller angle. Yet, the value is not quite different when the angle is 30°, 20°, 10° or 0°. The F_o decreases as much as 4% and the U_L increases as much 3.5% when the obstacles bent at 30 degree instead of 0 degree.

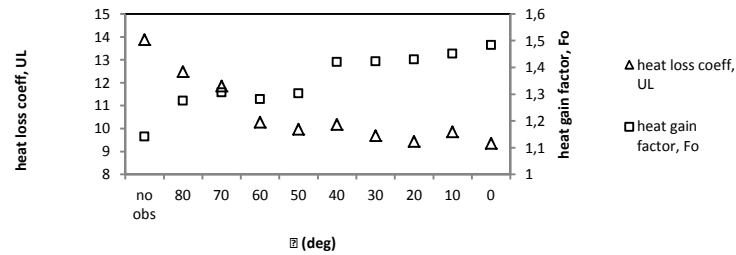


Fig. 6. The heat loss coefficient and heat gain factor of SAH with many configurations.

Conclusion

In the experimental study conducted, ten configuration of SAH were observed and compared. Following conclusions can be drawn:

- Obstacles placed on the bottom plate in a SAH with v-corrugated absorber plate improve the SAH performance. Both the air temperature rise and efficiency increase with inserting obstacles bent at any angle vertically. Unfortunately, the pressure drop is increasing, too.
- Obstacles bent vertically at smaller angles (means more straight) give higher air temperature rise and efficiency. However, the optimum angle is found 30° . The air temperature rise and efficiency will be 5.3% lower when the obstacles bent 30° instead of 0° , but the pressure drop will be 17.2% lower.

Acknowledgement

Here, I am very grateful for the support from Kopertis Wilayah VII Jawa Timur, Kementerian Pendidikan dan Kebudayaan by providing Research Grant under contract no: 0004/SP2H/PP/K7/KL/II/2012.

References

- [1] L. Tao, X. L. Wen, F. G. Wen and X. L. Chan, "A Parametric study on the thermal performance of a solar air collector with a V-groove absorber," *Int. J. of Green Energy*, 4, p. 601–622, 2007.
- [2] M. A. Karim and M. N. A. Hawlader, "Performance Investigation of Flat Plate, V-Corrugated and Finned Air Collector," *Energy* 31, pp. 452–470, 2006.
- [3] C. Choudhury and H. P. Garg, "Design Analysis of Corrugated and Flat Plate Solar Air Heaters," *Renewable Energy Vol I, No. 5/6*, p. p. 595 – 607, 1991.
- [4] A. A. Bashria, N. M. Adam, S. M. Sapuan and M. Daud, "Prediction Of The Thermal Performance Of Solar Air Heaters By Internet-Based Mathematical Simulation," *Proc. of the Institution of Mechanical Engineers*, p. 579 – 587, 2004.
- [5] P. Naphon, "Heat transfer characteristics and pressure drop in channel with V corrugated upper and lower plates," *Energy conversion and management* 48, p. 1516 – 1524, 2007.
- [6] Y. Islamoglu and C. Parmaksizoglu, "The effect of channel height on the enhanced heat transfer characteristics in a corrugated heat exchanger channel," *Applied Thermal Engineering* 23, p. 979–987, 2003.
- [7] P. Promvonge, "Heat transfer and pressure drop in a channel with multiple 60° V-baffles," *Int. Com. in Heat and Mass Transfer*, vol. 37, p. 835–840, 2010.
- [8] I. Kurtbas and E. Turgut, "Experimental Investigation of Solar Air Heater with Free and Fixed Fins: Efficiency and Exergy Loss," *Int. J. of Science & Technology*, vol. Volume 1, no. No 1, pp. 75–82., 2006.
- [9] B. S. Romdhane, "The air solar collectors: Comparative study, introduction of baffles to favor the heat transfer," *Solar Energy*, vol. 81, p. 139 – 149, 2007.
- [10] C.-D. Ho, H.-M. Yeh and T.-C. Chen, "Collector efficiency of upward-type double-pass solar air heaters with fins attached," *Int. Com. in Heat and Mass Transfer*, vol. 38, p. 49–56, 2011.

- [11] A. Abene, V. Dubois, M. Le Ray and A. Oagued, "Study of a solar air flat plate collector: use of obstacle and application for the drying of grape," *J. of Food Engineering*, vol. 65, p. 15 – 22, 2004.
- [12] H. Esen, "Experimental energy and exergy analysis of a double-flow solar air heater having different obstacles on absorber plates," *Building and Environment*, vol. 43, p. 1046–1054, 2008.
- [13] E. K. Akpınar and F. Koçyiğit, "Experimental investigation of thermal performance of solar air heater having different obstacles on absorber plates," *Int. Com. in Heat and Mass Transfer*, vol. 37, p. 416–421, 2010.
- [14] A. Bekele, M. Mishra and S. Dutta, "Effects of Delta-Shaped Obstacles on the Thermal Performance of Solar Air Heater," *Hindawi Publishing Corporation: Advances in Mechanical Engineering*, vol. 2011, p. 10 pages, 2011.
- [15] J. A. Duffie and W. A. Beckman, *Solar Engineering Of Thermal Processes*, 2nd ed., John Wiley & Sons, Inc., 1991.

Advances in Applied Mechanics and Materials

10.4028/www.scientific.net/AMM.493

Experimental Studies on a Solar Air Heater Having V-Corrugated Absorber Plate with Obstacles Bent Vertically

10.4028/www.scientific.net/AMM.493.86